

# Parameter calibration and experimental verification of discrete element simulation model for *Protaetia brevitarsis* larvae bioconversion mixture

Yuanze Li<sup>1,2</sup>, Jianhua Xie<sup>1,2\*</sup>, Jia Zhang<sup>1,2</sup>, Yong Yue<sup>1,2</sup>, Qinghe Meng<sup>1,2</sup>, Yakun Du<sup>1,2</sup>, Deying Ma<sup>1</sup>

(1. College of Mechanical and Electrical Engineering, Xinjiang Agricultural University, Urumqi 830052, China;

2. Key Laboratory of Xinjiang Intelligent Agricultural Equipment, Xinjiang Agricultural University, Urumqi 830052, China)

**Abstract:** To improve the survival rate of larvae during material separation after biotransformation of existing residual film mixtures of *Protaetia brevitarsis* larvae, this paper adopts the method of combining physical test and EDEM simulation test, and selects Hertz Mindlin with JKR contact model to calibrate the discrete element simulation contact parameters of the *Protaetia brevitarsis* larvae and the frass mixture. First, the cylinder lifting method was used to determine the actual repose angle of the mixture of larvae and frass. The collision recovery coefficients between larvae-frass and steel, static friction coefficient, kinetic friction coefficient and the collision recovery coefficient between larvae were measured through physical tests such as the inclined plane method. The Plackett-Burman test was then used to screen out the factors that have a significant impact on the repose angle: Poisson's ratio of frass, frass-frass rolling friction coefficient, frass JKR surface energy, frass-larvae JKR surface energy. The optimal value intervals of four significant factors were determined based on the steepest climb test. Based on the Box-Behnken response surface analysis test, the second-order regression model between the repose angle and four significant factors was determined, and variance and interaction effects were analyzed. And with the actual repose angle as the goal, the significant factors were optimized and the optimal parameter combination of the four significant factors was determined. The simulation test of material repose angle and screening was carried out with the optimal parameter combination, and compared with the physical test. It was found that the maximum relative errors of the two tests were 1.48% and 3.79% respectively, indicating that the calibrated parameter values are true and reliable. It can provide a reference for the discrete element simulation of the transportation and separation of the *Protaetia brevitarsis* larvae-frass mixture.

**Keywords:** *Protaetia brevitarsis* larvae-frass mixture, repose angle, parameter calibration, discrete element, model

**DOI:** [10.25165/j.ijabe.20241704.8707](https://doi.org/10.25165/j.ijabe.20241704.8707)

**Citation:** Li Y Z, Xie J H, Zhang J, Yue Y, Meng Q H, Du Y K, et al. Parameter calibration and experimental verification of discrete element simulation model for *Protaetia brevitarsis* larvae bioconversion mixture. *Int J Agric & Biol Eng*, 2024; 17(4): 35–44.

## 1 Introduction

Due to the large impurity content in the current residual film recovery mixture, it is difficult to separate the residual film from straw and crushed soil. People have developed a large number of membrane separation machinery. However, the separation effect of straw, stubble and residual film in impurities is not good, and the economic benefit is low<sup>[1,2]</sup>. In recent years, the research on the bioconversion of agricultural wastes by insects has attracted more and more attention. The investigation found that the larvae of *Protaetia brevitarsis* belong to saprophagous insects. Throughout the

larval stage, they feed on straw in the residual film mixture after fermentation<sup>[3]</sup>, the use of the insect can solve the problem that the residual film is difficult to separate from the straw and the root stubble. The materials after the insect transforms the residual film mixture include frass, the larvae itself and the residual film. Among them, frass can be used directly as organic fertilizer, the larvae themselves can be used as medicine, protein feed, etc. It has created huge economic benefits for farmers<sup>[4]</sup>. However, the existing research at home and abroad focuses on the nutritional components of the larvae, their own growth parameters, and their ability to deal with agricultural waste<sup>[5,6]</sup>. There is little research on the material transportation and screening process after the *Protaetia brevitarsis* larvae bioconversion the residual film mixture. After *Protaetia brevitarsis* larvae bioconversion the residual film mixture, the characteristics of the larvae and frass in the material are complex. It is difficult to accurately obtain relevant physical parameters using conventional methods. Therefore, this article has chosen to use the discrete element method to perform virtual calibration of the *Protaetia brevitarsis* larvae-frass mixture. In order to provide help for the optimization and improvement of subsequent material conveying and screening devices.

With the development of computer numerical simulation technology, discrete element method is widely used in agricultural technology and equipment. In the process of applying discrete element method simulation to optimize and improve the existing device, the intrinsic parameters and contact parameters of materials are very important. Because some parameters are difficult to obtain

**Received date:** 2023-12-06 **Accepted date:** 2024-06-12

**Biographies:** Yuanze Li, MS, research interest: agricultural solid waste recycling machinery and equipment, Email: [2368476220@qq.com](mailto:2368476220@qq.com); Jia Zhang, PhD, Associate Professor, research interest: agricultural solid waste recycling machinery and equipment, Email: [zj34@xjue.edu.cn](mailto:zj34@xjue.edu.cn); Yong Yue, Associate Professor, research interest: agricultural solid waste recycling machinery and equipment, Email: [xndyueyong@126.com](mailto:xndyueyong@126.com); Qinghe Meng, MS, research interest: agricultural solid waste recycling machinery and equipment, Email: [1452768668@qq.com](mailto:1452768668@qq.com); Yakun Du, MS, research interest: agricultural solid waste recycling machinery and equipment, Email: [2798004279@qq.com](mailto:2798004279@qq.com); Deying Ma, Professor, research interest: green prevention and control of pests, Email: [mdyxnd@163.com](mailto:mdyxnd@163.com).

\*Corresponding author: Jianhua Xie, Professor, research interest: agricultural solid waste recycling machinery and equipment. College of Mechanical and Electrical Engineering, Xinjiang Agricultural University, No.311, Nongda East Road, Urumqi 830052, China. Tel: +86-13325577846, Email: [xjh199032@163.com](mailto:xjh199032@163.com).

through conventional tests, scholars at home and abroad have proposed a method for virtual calibration of materials based on discrete element method. Peng et al.<sup>[7,8]</sup> combined discrete element simulation with repose angle test. The organic fertilizer and the intrinsic parameters and contact parameters of the black soldier fly after the treatment of pig manure were calibrated. Sun et al and Barr et al.<sup>[9,10]</sup> calibrated the contact model parameters of soil and soil-engaging parts. Based on the repose angle test, Zhu et al.<sup>[11]</sup> determined the discrete element parameters of sheep manure under different water contents. Tian et al.<sup>[12]</sup> carried out discrete element simulation and calibrated relevant parameters with corn straw and soil mixture as the research object. Yuan et al.<sup>[13]</sup> selected Hertz-Mindlin with Johnson-Kendall-Roberts contact model to calibrate the parameters of machine-applied organic fertilizer. Song et al.<sup>[14]</sup> Taking mulberry soil as an example, they calibrated the simulation parameters of soil particles. The research of the above authors verifies the feasibility of using discrete element method to obtain the intrinsic parameters and contact parameters of granular materials. However, there are few reports on the parameter calibration of the discrete element simulation model for the larvae and its frass.

In this paper, the *Protaetia brevitarsis* larva-frass mixture is taken as the research object. Through the combination of physical test and simulation test, the intrinsic parameters and contact parameters of the *Protaetia brevitarsis* larva-frass mixture are calibrated by EDEM software. Taking the repose angle as the response value, Hertz-Mindlin with JKR is selected as the contact model, The Plackett-Burman design test, the steepest climbing test and the Box-Behnken test were used to obtain the optimal discrete element simulation model parameters of *Protaetia brevitarsis* larva-frass mixture. It provides a reference for the movement state of the larva-frass mixture transportation and screening link of *Protaetia brevitarsis*.

## 2 Materials and methods

### 2.1 Test materials

The *Protaetia brevitarsis* larva-frass mixture used in this paper was provided by the Insect Industrialization Research Base of Manas County, Xinjiang, as shown in Figure 1. Since the residual film is a flexible sheet material, its levitation speed is small, and most of them are separated by air separation. When the mixture of *Protaetia brevitarsis* larvae, frass and residual film enters the screening device, the residual film is screened out by the air flow, basically does not participate in the subsequent screening process of frass and larvae. Therefore, this article chooses the white star beetle larva-frass mixture as the research object. After testing, it was found that the mass ratio of *Protaetia brevitarsis* larvae to frass was 1:9 (a few impurities in the mixture are treated as frass). The densities of frass and *Protaetia brevitarsis* larvae were  $940 \text{ kg/m}^3$  and  $412 \text{ kg/m}^3$  respectively. The moisture content of frass was 52%.



Figure 1 Samples test materials

### 2.2 Test method

In this paper, the parameters of the discrete element model of the larva-frass mixture were calibrated by the combination of physical test and EDEM simulation test. The actual repose angle of the larva-frass mixture was obtained by cylinder lifting method. Matlab software was used to process the image of the repose angle of the larva-frass mixture to obtain the actual value<sup>[15-17]</sup>. EDEM2020 software was selected to carry out the simulation experiment of repose angle. Plackett-Burman screening test was designed by Design-Expert11 software. The parameters that have significant influence on the repose angle were selected. According to the steepest climbing test, the optimal value interval of the significant parameters was determined. The Box-Behnken test was used to establish and optimize the regression model of the repose angle and significance parameters of the larva-frass mixture of *Protaetia brevitarsis*, and the optimal parameters combination was obtained. The simulation test of repose angle was carried out by the optimal parameter combination, the relative error between the simulated repose angle and the actual repose angle was compared, and the accuracy of the parameter calibration of the discrete element model for the *Protaetia brevitarsis* larva-frass mixture was verified.

### 2.3 Repose angle physical test

As shown in Figure 2. The cylinder lifting method was used to test the physical repose angle of the larva-frass mixture. The ratio of the inner diameter to the height of the steel cylinder is 1:2, the height of the cylinder is 180 mm, and the bottom of the cylinder is in contact with the steel plate. The cylinder is evenly filled with 300 g of the mixture of the larvae and the frass (frass 270 g, larvae 30 g). Among them, because the larvae of *Protaetia brevitarsis* are physical models in EDEM software simulation, morphological changes cannot occur. In order to reduce the experimental error, all physical experiments in this study selected the larvae of *Protaetia brevitarsis* after shaking. The WDW-50 M universal testing machine was used to lift the cylinder at a speed of 500 mm/min. The mixture flows out from the bottom of the cylinder and contacts with the steel plate. After the mixture pile is stabilized, the front view image of the mixture pile is taken by camera. The front view image of the mixed pile is imported into Matlab R2021b software for grayscale processing, binarization processing, hole filling, and boundary contour extraction. The contour map is imported into Origin2019b software, and the coordinate values of each point of the contour are obtained through its digital processing tool Digitize, and then the contour coordinate values are transformed into a dotted line graph and linearly fitted, as shown in Figure 3. In order to reduce the error, the average value of the repose angle on both sides of the mixed pile is selected as the measured value of the repose angle<sup>[18]</sup>.

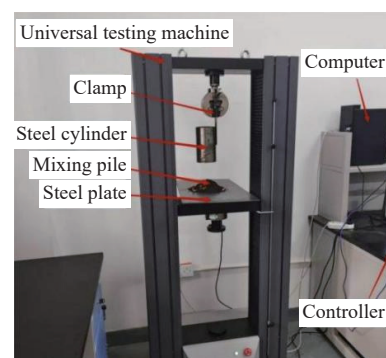


Figure 2 Physical test of the repose angle

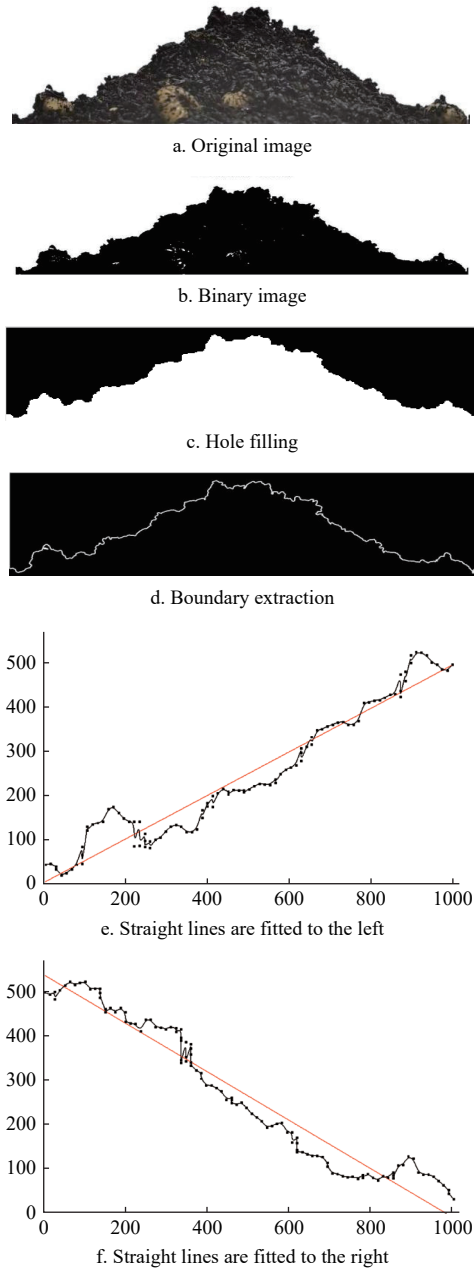


Figure 3 Repose angle image processing

The linear fitting equations of the two sides of the larvae-frass mixture are as follows:

$$Y_L = 0.508x + 1.395 \quad (R^2 = 0.941) \quad (1)$$

$$Y_R = -0.541x + 534.393 \quad (R^2 = 0.943) \quad (2)$$

where,  $Y$  is contour pixel point ordinate;  $x$  is Contour pixel abscissa.

$$\alpha = \frac{\arctan|K_L| + \arctan|K_R|}{2} \quad (3)$$

where,  $\alpha$  is the repose angle of the *Protaetia brevitarsis* larvae-frass mixture;  $K$  is the slope of the contour fitting straight line.

According to the Equations (1)-(3), the repose angle of the larvae-frass mixture was 27.67°.

### 3 Parametric measurement

#### 3.1 Determination of contact parameters between larvae-frass and steel

##### 3.1.1 Coefficient of static friction

The maximum static friction force of the material is

proportional to the positive pressure between the contact surfaces, and its proportional coefficient is called the static friction coefficient<sup>[19]</sup>. As shown in Figure 4, the slope sliding test was used to determine the static friction coefficient between the larvae-frass and the material plate. Because the main material of the transportation and screening device of the larvae-frass mixture was steel, the material plate was steel plate. During the test, the steel plate was placed horizontally on the angle adjustment device, and the larvae of *Protaetia brevitarsis* were placed on the steel plate. The angle adjustment device was slowly adjusted to make the steel plate rotate slowly along its side, Until the larvae began to slide down along the steel plate, the electronic protractor was used to measure the inclination angle of the steel plate<sup>[20]</sup>, and the average inclination angle was calculated after 20 times of repeated tests, According to Equation (4), the static friction coefficient between the larvae and the steel plate can be obtained.

$$\mu = \tan \theta \quad (4)$$

where,  $\mu$  is static friction coefficient of white spotted turtle larvae-steel plate;  $\theta$  is critical angle of static friction coefficient, (°).

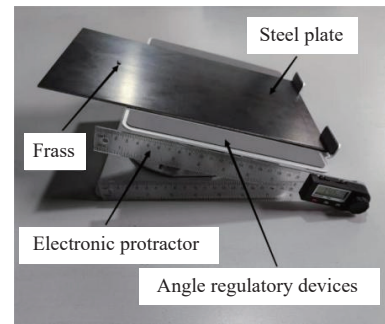


Figure 4 Static friction coefficient measurement device

When measuring the static friction coefficient between the frass and the steel plate, it is only necessary to replace the frass with the larvae. Among them, because the frass is a granular material and the particle size is small, in order to avoid the rolling of the frass during the measurement and increase the experimental error, four frass were bonded together for measurement during the test. The test results are listed in Table 1.

Table 1 Calculation results of the static friction coefficient

Material quality	Critical angle/(°)	Coefficient of static friction
<i>Protaetia brevitarsis</i> larvae-steel plate	18.0	0.325
Frass-steel plate	32.0	0.625

##### 3.1.2 Coefficient of rolling friction

The rolling friction coefficient refers to the ratio of the rolling friction torque to the normal load of the material<sup>[21]</sup>. As shown in Figure 5, the rolling friction coefficient between the larvae-frass and steel plate was measured by inclined rolling test, In the experiment, the steel plate was placed horizontally on the angle adjustment device, and the larvae of the *Protaetia brevitarsis* were placed on the steel plate, The angle adjustment device was slowly adjusted to make the steel plate rotate slowly along its side until the larvae of the *Protaetia brevitarsis* had a rolling trend, The electronic protractor was used to measure the inclination angle of the steel plate, and the average inclination angle was calculated after 20 repeated tests. According to Equations (5)-(8), the rolling friction coefficient between the larvae and the steel plate can be calculated.

$$\sigma = \frac{M}{F_n} \quad (5)$$

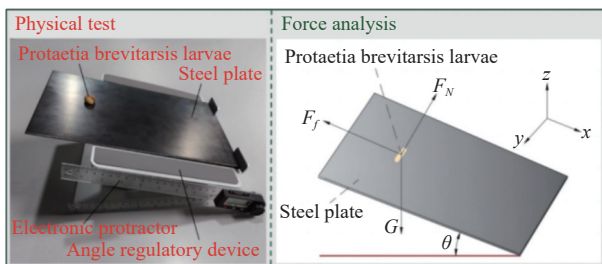


Figure 5 Rolling friction coefficient measuring device and force analysis diagram

$$F_N = G \cos \theta_1 \tag{6}$$

$$M = Gr \sin \theta_1 \tag{7}$$

$$f = \frac{M}{F_N} = r \tan \theta_1 \tag{8}$$

where,  $\sigma$  is coefficient of rolling friction;  $M$  is moment of rolling friction, N·m;  $F_N$  is the support of steel plate to the larvae of *Protaetia brevitarsis*, N;  $G$  is Gravity of *Protaetia brevitarsis* larvae, N;  $\theta_1$  is Critical angle of rolling friction coefficient, ( $^\circ$ );  $r$  is larvae radius of *Protaetia brevitarsis*, mm.

To measure the coefficient of rolling friction between the frass and the steel plate, it is only necessary to replace the *Protaetia brevitarsis* larvae with frass, and the test results are listed in Table 2.

Table 2 Calculation results of the rolling friction coefficient

Material quality	Critical angle/( $^\circ$ )	Coefficient of rolling friction
<i>Protaetia brevitarsis</i> larvae-steel plate	5.0	0.435
Frass-steel plate	9.5	0.167

### 3.1.3 Coefficient of restitution

The collision restitution coefficient is the ratio of the separation velocity to the approaching velocity of two objects along the normal direction of the contact surface before and after the collision, It is only related to the material of the collision object itself<sup>[21]</sup>. In this study, the free-fall collision test was used to determine the collision recovery coefficient between the larvae-frass mixture and the steel plate<sup>[23]</sup>. The test principle is shown in Figure 6. In the experiment, the steel plate was placed horizontally, so that the larvae of *Protaetia brevitarsis* could make a free fall motion from the height  $H$  of the steel plate. The larvae of *Protaetia brevitarsis* rebounded after colliding with the steel plate. The rebound height  $h$  of the larvae of *Protaetia brevitarsis* was recorded by OLYMPUS  $i$ -speed TR high-speed camera, and the average rebound height of the larvae of *Protaetia brevitarsis* was calculated after 20 repeated tests, According to Equation (9), the collision recovery coefficient between the larvae and the steel plate can be obtained.

$$e = \frac{v_0}{v_1} = \sqrt{\frac{h}{H}} \tag{9}$$

where,  $e$  is collision recovery coefficient between larvae of *Protaetia brevitarsis* and steel plate;  $v_0$  is the normal relative separation speed of *Protaetia brevitarsis* larvae and steel plate;  $v_1$  is the larvae of *Protaetia brevitarsis* are relatively close to the normal speed of the steel plate;  $h$  is rebound height of *Protaetia brevitarsis* larvae;  $H$  is falling height of *Protaetia brevitarsis* larvae.

When measuring the collision recovery coefficient between the frass and the steel plate, it is only necessary to replace the frass with the larvae of *Protaetia brevitarsis*. The test results are listed in Table 3.

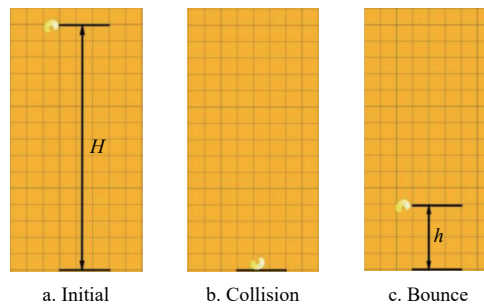


Figure 6 Free-fall crash test

Table 3 Calculation results of the collision recovery coefficient

Material quality	Coefficient of restitution
<i>Protaetia brevitarsis</i> larvae-steel plate	0.223
Frass-steel plate	0.387

### 3.2 Determination of larvae-frass and its own contact parameters

Due to the large error in the determination of the contact parameters between the larvae of *Protaetia brevitarsis* and the frass and the frass itself by the slope test and the free fall test, this study only used the fine line suspension test to determine the collision recovery coefficient between the larvae of *Protaetia brevitarsis*<sup>[24]</sup>. The remaining contact parameters are calibrated by EDEM simulation software.

As shown in Figure 7, the larvae  $a$  and  $b$  of *Protaetia brevitarsis* were tethered by fine lines, so that the larvae  $b$  of *Protaetia brevitarsis* was naturally suspended and kept stationary. The larvae  $a$  of *Protaetia brevitarsis was lifted to a certain fixed height and released, so that the two collided radially, After the collision, the larvae  $a$  and  $b$  of *Protaetia brevitarsis* continued to swing forward due to inertia. At this time, the maximum height of the swing of larvae  $a$  and  $b$  of *Protaetia brevitarsis* was recorded after 20 times of repeated experiments using a high-speed camera. According to Equation (10), the collision recovery coefficient between the larvae of *Protaetia brevitarsis* can be obtained.*

$$e_1 = \frac{\sqrt{H_2} - \sqrt{H_1}}{\sqrt{H_0}} \tag{10}$$

where,  $e_1$  is collision recovery coefficient between larvae of *Protaetia brevitarsis*;  $H_0$  is *Protaetia brevitarsis* larvae  $a$  lifting height;  $H_1$  is the swing height of larvae  $a$  of *Protaetia brevitarsis*;  $H_2$  is *Protaetia brevitarsis* larvae  $b$  swing height.

The test results are listed in Table 4.

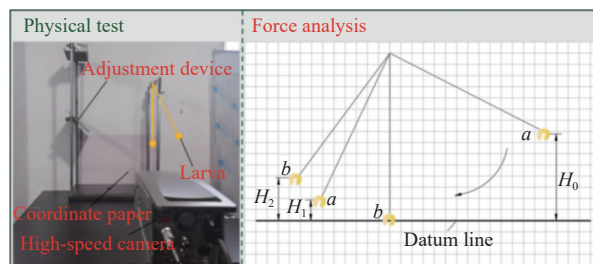


Figure 7 Schematic diagram of the collision recovery coefficient measurement

Table 4 Calculation results of the collision recovery coefficient

Material quality	Coefficient of restitution
Larvae-larvae	0.185

## 4 Simulation test of repose angle

### 4.1 Set up the simulation model

When selecting a contact model, because the *Protaetia brevitarsis* larvae-frass mixture itself has a certain humidity, it is easy to produce adhesion phenomenon. The Hertz-Mindlin with JKR contact model is suitable for powder particles and wet materials such as crops, ores, and soil, its simulation model particles are prone to obvious bonding and agglomeration<sup>[25]</sup>. Therefore, the Hertz-Mindlin with JKR contact model was selected for parameter calibration. The JKR contact model introduces surface energy into particle-particle interactions, its simplified model is shown in Figure 8. By screening and observing the mixture of *Protaetia brevitarsis* larvae and frass, the shape of frass is similar to a cylinder, while the larvae of *Protaetia brevitarsis* are curled up in the real conveying and screening state due to their biological stress. Therefore, combined with their respective sizes, it is finally determined that the frass is composed of three basic spheres with a radius of 1 mm, and the larvae of *Protaetia brevitarsis* are composed of seven basic spheres with a radius of 5 mm, as shown in Figure 9. The steel cylinder model was generated by three-dimensional software SolidWorks 2021 and imported into EDEM simulation software, The steel plate can be generated by EDEM simulation software itself, The Poisson's ratio of the steel is 0.30, the shear modulus is  $7.9 \times 10^4$  MPa, and the density is  $7.85 \times 10^3$  kg/m<sup>3</sup>.

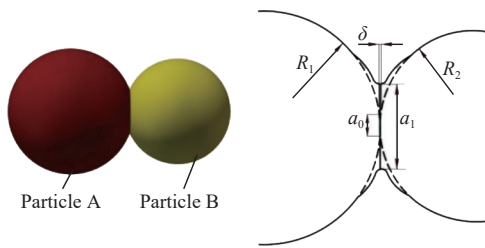


Figure 8 JKR contact model

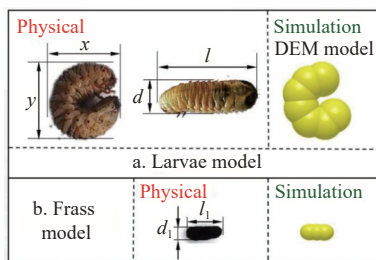


Figure 9 Material model

### 4.2 Setting of simulation parameters

In the simulation process of EDEM software, steel cylinders and steel plates with the same physical test parameters as the repose angle are imported. The time step was set to 22% of the Rayleigh time step. The data storage time interval was 0.01 s. The mesh size was set to 3 times the minimum particle radius. The particle generation method is Dynamic, a virtual Polygon plane is set above the steel cylinder as a particle factory<sup>[26]</sup>. Set the generation rate of frass to 135 g/s, and 12 larvae/s, (30 g about 24), and the generation time of both is set to 2 s. After the particles are stabilized, the steel cylinder begins to move vertically upward at a speed of 500 mm/min in 3 s until a stable repose angle is formed on the steel plate, as shown in Figure 10. Among them, the same method as the physical experiment can be used to reduce the error when measuring the repose angle of the simulation test.

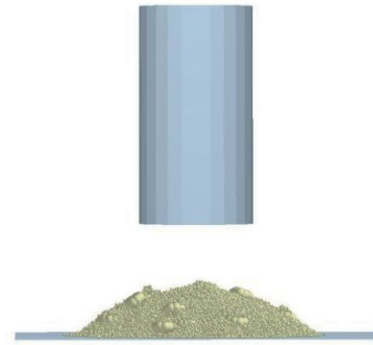


Figure 10 simulation test of repose angle

## 5 Test and result analysis

### 5.1 Plackett-Burman test

The Plackett-Burman test mainly analyzes each factor at two levels, and determines the significance of the factor by comparing the difference between the two levels of each factor and the overall difference. In this study, the Plackett-Burman test with  $N=19$  was designed by Design-Expert11, and four virtual items were set aside for error analysis. The repose angle of *Protaetia brevitarsis* larvae-frass mixture was used as the experimental index, The parameters that have a significant effect on the repose angle were screened from the frass (Poisson's ratio, shear modulus), the larvae of *Protaetia brevitarsis* (Poisson's ratio, shear modulus), the frass (static friction coefficient, rolling friction coefficient, collision recovery coefficient), the larvae of *Protaetia brevitarsis* (static friction coefficient, rolling friction coefficient), the frass and the larvae of *Protaetia brevitarsis* (static friction coefficient, rolling friction coefficient, collision recovery coefficient), JKR surface energy (frass, *Protaetia brevitarsis* larvae, frass and *Protaetia brevitarsis* larvae).

At present, the research on the conversion of the larvae of the *Protaetia brevitarsis* into the residual film recycling mixture of farmland is still in the primary stage, and the parameters of the discrete element simulation model are extremely scarce. Therefore, on the basis of a large number of experiments, referring to relevant literature, the parameters of the simulation model of the *Protaetia brevitarsis* larvae-frass mixture are determined as listed in Table 5.

Table 5 Discrete element simulation test factors and level

Symbols of factors	Factor	Level		
		-1	0	1
A	Poisson's ratio of frass	0.1	0.3	0.5
B	Poisson's ratio of larvae	0.2	0.3	0.4
C	Shear modulus of frass/ MPa	1	5	10
D	Shear modulus of larvae/ MPa	8	11	14
E	Static friction coefficient of frass-frass	0.1	0.55	1
F	Rolling friction coefficient of frass-frass	0.05	0.35	0.65
G	Collision recovery coefficient of frass-frass	0.1	0.35	0.6
H	Static friction coefficient of frass-larvae	0.3	0.6	0.9
J	Rolling friction coefficient of frass-larvae	0.2	0.5	0.8
K	Collision recovery coefficient of frass-larvae	0.1	0.25	0.4
L	Larval-larvae static friction coefficient	0.4	0.5	0.6
M	Larval-larvae rolling friction coefficient	0.3	0.4	0.5
N	JKR surface energy of larvae/J·m <sup>-2</sup>	0.05	0.35	0.65
O	JKR surface energy of frass/J·m <sup>-2</sup>	0	0.1	0.2
P	JKR surface energy of frass-larvae/J·m <sup>-2</sup>	0.1	0.4	0.7

The scheme and results of Plackett-Burman test are listed in Table 6. The data in Table 6 were analyzed using Design-Expert11

software, the Pareto diagram is shown in Figure 11. It can be seen from the Pareto chart that the effect of five factors on the repose angle is negative, that is, the repose angle increases with the decrease of the factor value. The five factors are: Shear modulus of frass (*C*), collision recovery coefficient of frass-frass (*G*), rolling friction coefficient of frass-larvae (*J*), collision recovery coefficient of frass-larvae (*K*), static friction coefficient of larvae-larvae (*L*). The effect of the remaining 12 factors on the repose angle is positive. The four factors that have a significant effect on the repose angle ( $p < 0.05$ ) are as follows: the Poisson's ratio of the frass (*A*), the rolling friction coefficient of the frass-frass (*F*), the JKR surface energy of the frass (*O*), and the JKR surface energy of the frass-larvae (*P*). It can be seen from Table 7, the total contribution rate of the four factors that have a significant impact on the repose angle is 86.95%. In particular, the surface energy (*O*) of frass JKR contributes 59.52% to the repose angle. It can be judged from the data that the moisture content of frass has the greatest impact on the repose angle.

**Table 6 Plackett-Burman test protocol and results**

Serial No.	Factor															Repose angle/(°)	
	A	B	C	D	E	F	G	H	J	K	L	M	N	O	P		Q
1	1	1	-1	-1	1	1	1	1	-1	1	-1	1	-1	-1	-1	-1	26.52
2	-1	1	1	-1	-1	1	1	1	1	-1	1	-1	1	-1	-1	-1	17.21
3	1	-1	1	1	-1	-1	1	1	1	1	-1	1	-1	1	-1	-1	32.59
4	1	1	-1	1	1	-1	-1	1	1	1	1	-1	1	-1	1	-1	28.56
5	-1	1	1	-1	1	1	-1	-1	1	1	1	1	-1	1	-1	1	29.22
6	-1	-1	1	1	-1	1	1	-1	-1	1	1	1	1	-1	1	-1	21.29
7	-1	-1	-1	1	1	-1	1	1	-1	-1	1	1	1	1	-1	1	28.03
8	-1	-1	-1	-1	1	1	-1	1	1	-1	-1	1	1	1	1	-1	38.28
9	1	-1	-1	-1	-1	1	1	-1	1	1	-1	-1	1	1	1	1	35.18
10	-1	1	-1	-1	-1	-1	1	1	-1	1	1	-1	-1	1	1	1	28.79
11	1	-1	1	-1	-1	-1	-1	1	1	-1	1	1	-1	-1	1	1	23.27
12	-1	1	-1	1	-1	-1	-1	-1	1	1	-1	1	1	-1	-1	1	20.04
13	1	-1	1	-1	1	-1	-1	-1	-1	1	1	-1	1	1	-1	-1	30.35
14	1	1	-1	1	-1	1	-1	-1	-1	-1	1	1	-1	1	1	-1	40.05
15	1	1	1	-1	1	-1	1	-1	-1	-1	-1	1	1	-1	1	1	27.66
16	1	1	1	1	-1	1	-1	1	-1	-1	-1	-1	1	1	-1	1	37.11
17	-1	1	1	1	1	-1	1	-1	1	-1	-1	-1	-1	1	1	-1	29.48
18	-1	-1	1	1	1	1	-1	1	-1	1	-1	-1	-1	-1	1	1	23.96
19	1	-1	-1	1	1	1	1	-1	1	-1	1	-1	-1	-1	-1	1	25.02
20	-1	-1	-1	-1	-1	-1	-1	-1	-1	-1	-1	-1	-1	-1	-1	-1	18.79

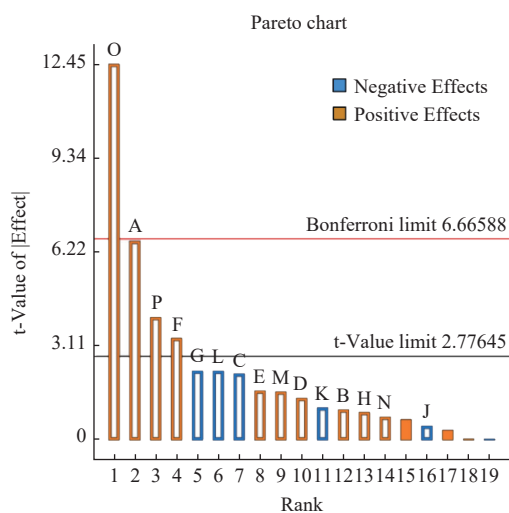


Figure 11 Pareto chart of Plackett-Burman experiment

**Table 7 Significance analysis of the Plackett-Burman test parameters**

Factor	Sum of squares	Stdized Effect	Contribution/%	F-value	p-value	Saliency list
Model	763.97	\	-	16.86	0.0072	-
A	131.17	5.12	16.68	43.43	0.0027**	2
B	3.10	0.79	0.395	1.03	0.3680	12
C	14.65	-1.71	1.86	4.85	0.0924	7
D	5.90	1.09	0.75	1.95	0.2349	10
E	8.14	1.28	1.04	2.70	0.1760	8
F	34.53	2.63	4.39	11.43	0.0278*	4
G	15.95	-1.79	2.03	5.28	0.0831	5
H	2.62	0.72	0.33	0.8676	0.4043	13
J	0.69	-0.37	0.09	0.2266	0.6589	15
K	3.53	-0.84	0.45	1.17	0.3406	11
L	15.88	-1.78	2.02	5.26	0.0836	6
M	7.81	1.25	0.99	2.59	0.1831	9
N	1.81	0.60	0.23	0.5999	0.4819	14
O	468.12	9.68	59.52	154.97	0.0002**	1
P	50.05	3.16	6.36	16.57	0.0152*	3

Note: \* indicates a significant impact ( $0.01 < p < 0.05$ ); \*\* indicates that the effect is extremely significant ( $p \leq 0.01$ ).

**5.2 Steepest ascent experiment**

According to the significance test results of Plackett-Burman test, combined with the significance of each factor and the order of contribution rate, four parameters that have a significant effect on the repose angle are selected: the Poisson's ratio of frass (*A*), the rolling friction coefficient of frass-frass (*F*), the JKR surface energy of frass (*O*), and the JKR surface energy of frass-larvae (*P*). The relative error of the repose angle between the physical experiment and the simulation experiment was used as the evaluation index to carry out the steepest climbing test. In the simulation parameter setting, the parameters with small contribution rate to the repose angle are taken as the intermediate level values, namely, the Poisson's ratio of larvae (*B*) 0.3, the shear modulus of frass (*C*) 5 MPa, the shear modulus of larvae (*D*) 11 MPa, the static friction coefficient of frass-frass (*E*) 0.55, the collision recovery coefficient of frass-frass (*G*) 0.35, the static friction coefficient of frass-larvae (*H*) 0.6, the rolling friction coefficient of frass-larvae (*J*) 0.5, the collision recovery coefficient of frass-larvae (*K*) 0.25, the static friction coefficient of larvae-larvae (*L*) 0.5, the rolling friction coefficient of larvae-larvae (*M*) 0.4, and the surface energy of larvae JKR (*N*) 0.35 J/m<sup>2</sup>. The test scheme and results are shown in Table 8. The relative error *Y* between the simulated repose angle  $\alpha_1$  and the actual repose angle  $\alpha$  can be calculated by Equation (11).

$$Y = \frac{|\alpha_1 - \alpha|}{\alpha} \tag{11}$$

**Table 8 Test scheme and results of the steepest climbing slope**

Serial No.	A	F	O	P	Repose angle/(°)	Relative error/(%)
1	0.10	0.05	0	0.10	25.31	8.53
2	0.20	0.20	0.05	0.25	25.81	6.72
3	0.30	0.35	0.10	0.40	28.39	2.60
4	0.40	0.50	0.15	0.55	30.97	11.93
5	0.50	0.65	0.20	0.70	33.10	19.63

The results show that with the increase of Poisson's ratio of frass (*A*), the rolling friction coefficient of frass-frass (*F*), the JKR surface energy of frass (*O*) and the JKR surface energy of frass-larvae (*P*), the simulation repose angle of the mixture of *Protactia brevitarsis* larvae-frass increases continuously, and the relative error

between the simulation test repose angle and the physical test repose angle decreases first and then increases. In particular, the relative error of the repose angle of the third group of tests is the smallest. Therefore, the third group of test parameter values was selected as the intermediate level, and the second group and the fourth group of tests are used as low and high levels respectively for subsequent Box-Behnken tests. The parameter levels are listed in Table 9.

**Table 9 Parameter level table**

Level	Factor			
	<i>A</i>	<i>F</i>	<i>O</i>	<i>P</i>
-1	0.20	0.20	0.05	0.25
0	0.30	0.35	0.10	0.40
1	0.40	0.50	0.15	0.55

**5.3 Box-Behnken test**

According to the results of the steepest climbing test, Design-Expert11 was used to design the response surface test of four factors and three levels, a total of 29 groups of tests were carried out, including 5 repeated tests at the intermediate level. The test design and results are listed in Table 10. The Box-Behnken test was subjected to multiple regression fitting analysis, and the second-order regression equation between the repose angle and the four factors was obtained as follows.

$$R = 29.56 + 0.1325A + 0.8642F + 1.86O + 0.7008P + 0.5175AF + 0.1650AO - 0.2550AP + 0.5625FO + 0.6025FP - 0.3850OP - 0.3050A^2 - 0.9375F^2 - 0.9525O^2 - 0.7525P^2 \tag{12}$$

The results of the analysis of variance of the quadratic regression model are listed in Table 11, and the regression model  $p < 0.0001$ . It can be seen that the relationship between the quadratic regression equation obtained from the test and the repose angle is very significant. The loss of fit term  $p = 0.3551 > 0.05$ , it can be seen that the loss of fit term is not significant compared with the pure error, that is, the fitting is better. The determination coefficient  $R^2 = 0.9834$ , the correction determination coefficient  $R^2_{adj} = 0.9668$ , both greater than 0.95 close to 1, the precision of the test is 28.3703, and the coefficient of variation is  $CV = 1.04\%$ . It can be seen that the accuracy of the regression model is high. It can be seen from the F value of the model that the influence of the four factors on the repose angle from small to large is the Poisson's ratio of the frass (*A*), the surface energy of the frass-larvae JKR (*P*), the rolling friction coefficient of the frass-frass (*F*), the surface energy of the frass JKR (*O*). From the P value of the model, it can be seen that *F*, *O*, *P*, *AF*, *FO*, *FP*, *F^2*, *O^2* and *P^2* have a very significant effect on the repose angle, *OP* and *A^2* have a significant effect on the repose angle, and *A*, *AO* and *AP* have no significant effect on the repose angle.

By removing the items (*A*, *AO*, *AP*) that have no significant effect on the repose angle, the quadratic regression model is optimized. The variance analysis of the optimized quadratic regression model is shown in Table 12. The test precision = 28.7745 is improved compared with that before optimization, and the credibility of the model is further increased. The optimized second-order regression equation is:

$$R = 29.56 + 0.8642F + 1.8592O + 0.7008P + 0.5175AF + 0.5625FO + 0.6025FP - 0.385OP - 0.305A^2 - 0.9375F^2 - 0.9525O^2 - 0.7275P^2 \tag{13}$$

**Table 10 Design and results of the Box-Behnken test**

Serial No.	Factor				Repose angle/(°)
	<i>A</i>	<i>F</i>	<i>O</i>	<i>P</i>	
1	0	1	0	1	30.47
2	-1	-1	0	0	27.93
3	0	1	1	0	30.54
4	1	0	-1	0	26.25
5	0	0	1	-1	29.51
6	0	0	0	0	29.32
7	0	0	-1	-1	25.02
8	1	1	0	0	29.83
9	0	0	0	0	29.48
10	-1	0	1	0	29.95
11	1	0	1	0	30.59
12	0	1	0	-1	27.54
13	0	0	-1	1	27.11
14	0	1	-1	0	25.99
15	-1	1	0	0	28.58
16	1	0	0	1	28.98
17	0	-1	0	-1	26.45
18	0	-1	1	0	28.21
19	-1	0	0	-1	27.55
20	1	0	0	-1	28.33
21	1	-1	0	0	27.11
22	0	0	1	1	30.06
23	-1	0	0	1	29.22
24	0	-1	0	1	26.97
25	0	-1	-1	0	25.91
26	0	0	0	0	29.84
27	-1	0	-1	0	26.27
28	0	0	0	0	29.81
29	0	0	0	0	29.35

**Table 11 ANOVA with quadratic regression models for Box-Behnken trials**

Source	Sum of squares	df	Mean square	F-value	p-value
Model	72.32	14	5.17	59.32	<0.0001**
<i>A</i>	0.2107	1	0.2107	2.42	0.1421
<i>F</i>	8.96	1	8.96	102.92	<0.0001**
<i>O</i>	41.48	1	41.48	476.35	<0.0001**
<i>P</i>	5.89	1	5.89	67.69	<0.0001**
<i>AF</i>	1.07	1	1.07	12.30	0.0035**
<i>AO</i>	0.1089	1	0.1089	1.25	0.2823
<i>AP</i>	0.2601	1	0.2601	2.99	0.1059
<i>FO</i>	1.27	1	1.27	14.53	0.0019**
<i>FP</i>	1.45	1	1.45	16.68	0.0011**
<i>OP</i>	0.5929	1	0.5929	6.81	0.0206*
<i>A^2</i>	0.6034	1	0.6034	6.93	0.0197*
<i>F^2</i>	5.70	1	5.70	65.47	<0.0001**
<i>O^2</i>	5.88	1	5.88	67.58	<0.0001**
<i>P^2</i>	3.43	1	3.43	39.43	<0.0001**
Residual	1.22	14	0.0871		
Lack of fit	0.9701	10	0.0970	1.56	0.3551
Pure error	0.2490	4	0.0622		
Cor total	73.53	28			

Note: \* indicates a significant impact ( $0.01 < p < 0.05$ ); \*\* indicates that the effect is extremely significant ( $p \leq 0.01$ ).

**Table 12 Analysis of variance by optimizing the quadratic regression model for Box-Behnken trials**

Source	Sum of squares	df	Mean square	F-value	p-value
Model	71.74	11	6.52	61.64	<0.0001**
<i>F</i>	8.96	1	8.96	84.70	<0.0001**
<i>O</i>	41.48	1	41.48	392.01	<0.0001**
<i>P</i>	5.89	1	5.89	55.71	<0.0001**
<i>AF</i>	1.07	1	1.07	10.12	0.0055**
<i>FO</i>	1.27	1	1.27	11.96	0.0030**
<i>FP</i>	1.45	1	1.45	13.72	0.0018**
<i>OP</i>	0.5929	1	0.5929	5.60	0.0301*
<i>A</i> <sup>2</sup>	0.6034	1	0.6034	5.70	0.0288*
<i>F</i> <sup>2</sup>	5.70	1	5.70	53.88	<0.0001**
<i>O</i> <sup>2</sup>	5.88	1	5.88	55.62	<0.0001**
<i>P</i> <sup>2</sup>	3.43	1	3.43	32.45	<0.0001**
Residual	1.80	17	0.1058		
Lack of fit	1.55	13	0.1192	1.92	0.2787
Pure error	0.2490	4	0.0622		
Cor total	73.53	28			

Note: \* indicates a significant impact ( $0.01 < p < 0.05$ ); \*\* indicates that the effect is extremely significant ( $p \leq 0.01$ ).

### 5.4 Interaction effect analysis of quadratic regression model

In this paper, the Design-Expert11 software was used to draw the response surface of the four-factor interaction repose angle, and the influence of the interaction between factors on the repose angle is further analyzed, as shown in Figure 12. It can be seen from Figure 12a, Compared with the Poisson's ratio (*A*) response surface curve of frass, there is no obvious fluctuation, and the response surface curve of the rolling friction coefficient (*F*) of frass-frass is slightly steeper, indicating that it has a more significant effect on the repose angle; It can be seen from Figure 12b, Compared with the rolling friction coefficient (*F*) of the frass-frass, the JKR surface energy (*O*) response surface curve of the frass is steeper, indicating that it has a more significant effect on the repose angle; It can be seen from Figure 12c, The response surface is a convex surface, indicating that the rolling friction coefficient (*F*) of the frass-frass and the surface energy (*P*) of the frass-larvae JKR have basically the same effect on the repose angle; It can be seen from Figure 12d, Compared with the surface energy (*P*) of frass-larvae JKR, the response surface curve of the surface energy (*O*) of frass JKR is steeper, indicating that it has a more significant effect on the repose angle.

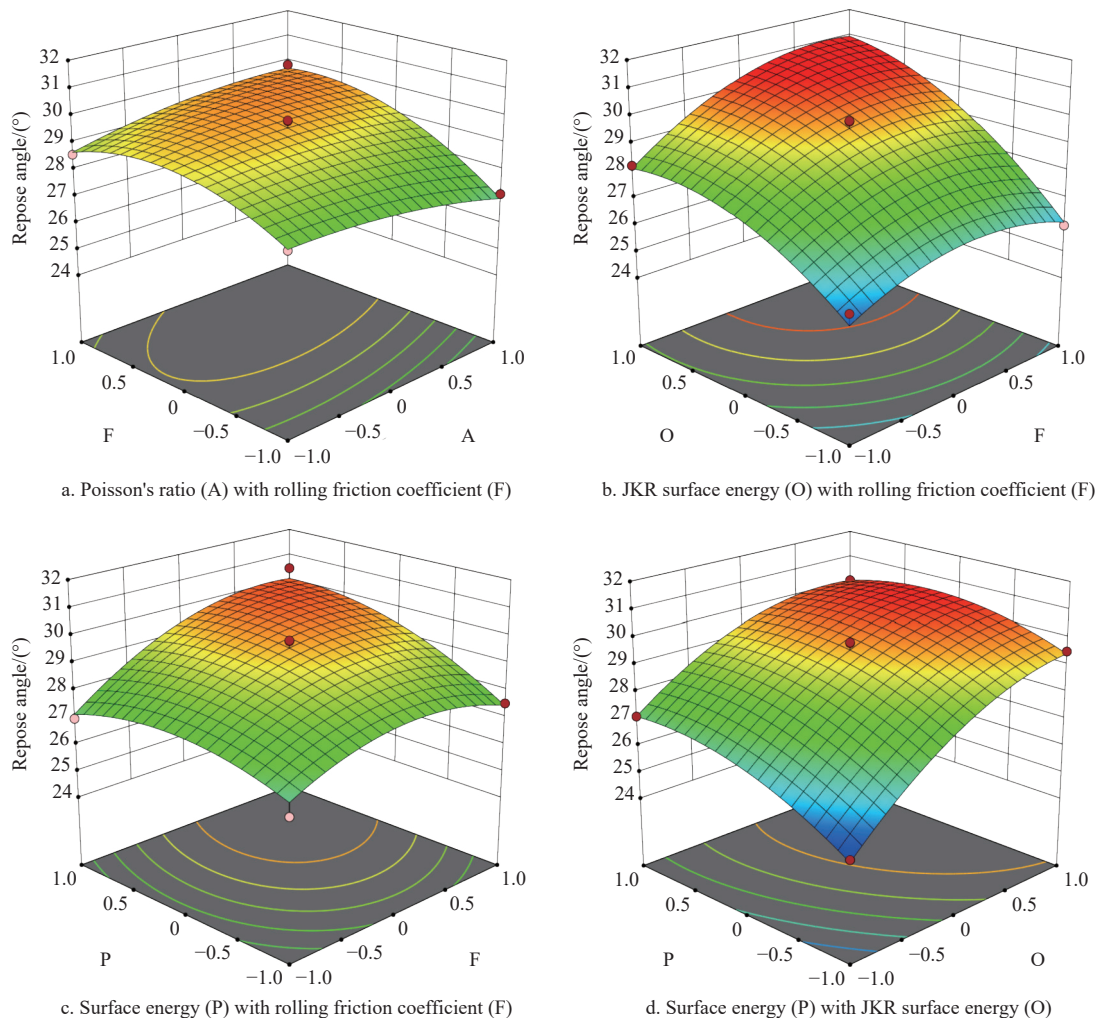


Figure 12 Response surface of factors interaction

### 5.5 Parameter optimization and repose angle test verification

Parameters were optimized through the Numerical module in Design-Expert11 software<sup>[27]</sup>. The regression equation was solved with the physical test repose angle of 27.67° as the goal, a set of parameter combinations closest to the target value were obtained,

As shown in Figure 13. Poisson's ratio (*A*) of frass was 0.290, the rolling friction coefficient (*F*) of frass-frass was 0.226, the JKR surface energy (*O*) of frass was 0.083, and the JKR surface energy (*P*) of frass-larvae was 0.425. The remaining non-significant parameters were averaged. In order to verify the true reliability of

the discrete element simulation, the optimized parameters were selected for three simulation tests, and the repose angle were 28.67°, 27.35° and 28.21°, respectively. The average value was 28.08°, and the relative error of the repose angle with the physical test was 1.48%, which verified the true reliability of the discrete element simulation. The test comparison is shown in Figure 14.

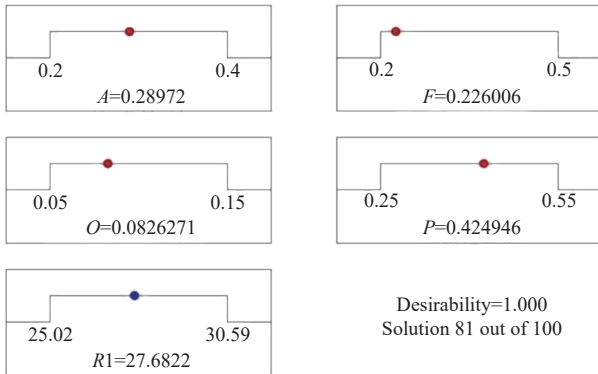


Figure 13 Optimization Results

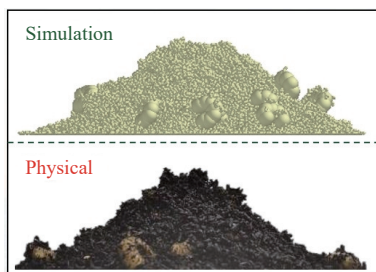


Figure 14 Comparison between simulation test and physical test

5.6 Screening test verification

The main moving parts (Figure 15) of the material screening prototype were modeled based on the structural parameters of the material screening prototype. Imported the model into the EDEM software and set its material to Q235 steel. When conducting a screening simulation test (Figure 16), the physical parameters of particles and contact materials were set according to the previously determined values. In order to reduce simulation time, the total set material was 2 kg (frass 1.8 kg, larvae 0.2 kg). The feeding speed was set to 2 kg/s, the rotation speed of the trommel screen was set to 6 r/min, the angle was set to 2°.



Figure 15 Material screening device

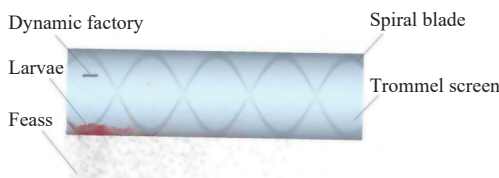


Figure 16 Material screening simulation test

During the real material screening test, it was found that 2 kg of material can be screened in only about 13 s. Therefore, set the simulation time to 15 s. Considering the existence of random errors, a total of 5 material screening tests were conducted<sup>[28]</sup>. Count and record the time it takes to screen 2 kg of material each time and calculate its relative error. The data comparison between the simulation test and the physical test is listed in Table 13. The maximum relative error between the physical value and the simulation value of the frass screening completion time does not exceed 5%, indicating that the calibration parameters are relatively accurate. It can provide help for the device design of the transportation and separation of *Protaetia brevitarsis* larvae and frass.

Table 13 Comparison of simulation and physical experiments

Number of trials	1	2	3	4	5
Simulation screening time/s	12.7	13.3	13.2	13.3	12.5
Physical screening time/s	13.2	13.6	12.8	13.5	12.8
Relative error	3.79	2.22	3.13	1.48	2.34

6 Conclusions

This article used high-speed camera technology and physical test methods such as inclined planes, free-fall collisions, and suspension collisions to determine the specific values of some friction coefficients and recovery coefficients. For parameters that are difficult to determine using physical experiments, this article determines their value ranges by reviewing the literature. The repose angle of the *Protaetia brevitarsis* larvae-frass mixture was measured using a universal testing machine. Used the repose angle as the response value, the Plackett-Burman test, the steepest climb test and the Box-Behnken response surface analysis test were used to significantly analyze, screen and optimize the physical parameters of the *Protaetia brevitarsis* larvae-frass mixture. A repose angle simulation model was established with optimized parameters and compared with the physical test repose angle to verify the accuracy of the calibrated parameters. Processed and produced a prototype for material screening after the white star beetle larvae transform the residual film mixture. Processed and produced a prototype for screening materials after *Protaetia brevitarsis* larvae transform residual film mixture, the main moving parts were selected to build a discrete element simulation model for screening materials. It was compared with the screening test of the physical prototype to ensure that the calibrated parameters can simulate the real screening situation. The specific conclusions of this study are as follows:

(1) Plackett-Burman test results show that: Poisson’s ratio of frass (*A*), the rolling friction coefficient of frass-frass (*F*), the JKR surface energy of frass (*O*) and the JKR surface energy of frass-larvae (*P*) of larvae-frass has a significant influence on the repose angle of the *Protaetia brevitarsis* larvae-frass mixture, the other parameters have no significant impact on the repose angle.

(2) The steepest climbing test and Box-Behnken response surface analysis test results show that: The repose angle regression model established in this article has good precision and accuracy. The optimal parameter combination of the *Protaetia brevitarsis* larvae-frass mixture is Poisson’s ratio (*A*) of frass is 0.290, Rolling friction coefficient (*F*) of frass-frass is 0.226, The JKR surface energy (*O*) of frass is 0.083, the JKR surface energy (*P*) of frass-larvae is 0.425, the remaining non-significant parameters are averaged.

(3) The repose angle comparison test shows that: The relative error between the simulated repose angle and the physical repose angle is 1.48%, it shows that the calibrated parameter values are highly accurate and can be used to simulate real screening situations.

(4) Screening comparison tests show that: The screening status of the simulation test and the physical test are close, it can be used for subsequent kinematics and dynamics simulation analysis of the material screening process after the *Protaetia brevitarsis* larvae transforms the residual film mixture.

In summary, this study used the straw-eating characteristics of *Protaetia brevitarsis* larvae to solve the problem of difficult separation of film stalks after mechanical recycling of residual film, hope to find a new way out for the current situation of difficult residual film mixture separation. The determination of the parameter values of the *Protaetia brevitarsis* larvae-frass mixture simulation model will provide a reference for the movement status of subsequent material transportation and separation links in this research direction.

## Acknowledgements

We acknowledge that his work was financially supported by the Autonomous Region Key R&D Program of Xinjiang, China (Grant No. 2022B02046).

## [References]

- [1] Shi X, Niu C H, Qiao Y Y, Zhang H C, Wang X N. Application of plastic trash sorting technology in separating waste plastic mulch films from impurities. *Transactions of the CSAE*, 2016; 32(Z2): 22–31. (in Chinese)
- [2] Zhou M D, Qin X H, Hou H, Yue Y B. Policy and present situation of pollution treatment of recycled plastic film in agricultural fields in Xinjiang. *Environment and Sustainability*, 2014; 39(5): 171–174. (in Chinese)
- [3] Yi H F, Wang Y, Ma Y X, Wang J S. Study on bio transformation of nutrients in corn stalks by larvae of *Protaetia brevitarsis*. *Special Economic Animals and Plants*, 2021; 24(12): 3–5. (in Chinese)
- [4] Yang C, Liu Y S, Xu X Y, Zhang J W. Analysis and evaluation of resource components of *Protaetia brevitarsis* (Lewis) Larvae. *Journal of Shandong Agricultural University*, 2014; 45(2): 166–170. (in Chinese)
- [5] Li P P. Study on the conversion ability of livestock and poultry manure using *Protaetia brevitarsis*. Shandong Agricultural University, 2022. (in Chinese)
- [6] Lai D Q, Wang Q L, Wu Y, Shu C L, Zhang Y, Liu C Q. Effect of *Protaetia brevitarsis* (Lewis) Larvae dung on development of pepper seedling stage under low temperature. *Northern Horticulture*, 2019; 431(8): 63–66. (in Chinese)
- [7] Peng C W, Xu D J, He X, Tang Y H, Sun S L. Parameter calibration of discrete element simulation model for pig manure organic fertilizer treated with *Hermetia illucen*. *Transactions of the CSAE*, 2020; 36(17): 212–218. (in Chinese)
- [8] Peng C W, Zhou T, Sun S L, Xie Y L, Wei Y. Calibration of parameters of black soldier fly in discrete method simulation based on response angle of particle heap. *Acta Agriculturae Zhejiangensis*, 2022; 34(4): 814–823. (in Chinese)
- [9] Sun J, Wang Y, MA Y, Tong J, Zhang Z. DEM simulation of bionic subsoilers (tillage depth>40 cm) with drag reduction and lower soil disturbance characteristics. *Advances in Engineering Software*, 2018; 119(5): 30–37.
- [10] Barr J B, Ucgul M, Desbiolles J M A, Fielke J M. Simulating the effect of rake angle on narrow opener performance with the discrete element method. *Biosystems Engineering*, 2018; 171(1): 1–15.
- [11] Zhu X H, Fu S K, Li X D, Wei Y Q, Zhao W. General method for discrete element parameters calibration of goat manure with different moisture contents. *Transactions of the CSAM*, 2022; 53(8): 34–41. (in Chinese)
- [12] Tian X L, Cong X, Qi J T, Guo H, Li M, Fan X H. Parameter calibration of discrete element model for corn straw-soil mixture in black soil areas. *Transactions of the CSAM*, 2021; 52(10): 100–108, 242. (in Chinese)
- [13] Yuan Q C, Xu L M, Xing J J, Duan Z Z, Ma S, Yu C C, Chen C. Parameter calibration of discrete element model of organic fertilizer particles for mechanical fertilization. *Transactions of the CSAE*, 2018; 34(18): 21–27. (in Chinese)
- [14] Song Z H, Li H, Yan Y F, Tian F Y, Li Y D, Li F D. Calibration method of contact characteristic parameters of soil in mulberry field based on unequal-diameter particles DEM theory. *Transactions of the CSAM*, 2022; 53(6): 21–33. (in Chinese)
- [15] Zhang W X, Wang F Y. Parameter calibration of American ginseng seeds for discrete element simulation. *Int J Agric & Biol Eng*, 2022; 15(6): 16–22.
- [16] Jia H L, Deng J Y, Deng Y L, Chen T Y, Wang G, Sun Z J, Guo H. Contact parameter analysis and calibration in discrete element simulation of rice straw. *Int J Agric & Biol Eng*, 2021; 14(4): 72–81.
- [17] Liang R Q, Chen X G, Zhang B C, Wang X Z, Kan Z, Meng H W. Calibration and test of the contact parameters for chopped cotton stems based on discrete element method. *Int J Agric & Biol Eng*, 2022; 15(5): 1–8.
- [18] Wang L M, Fan S Y, Cheng H S, Meng H B, Shen Y J, Wang J, et al. Calibration of contact parameters for pig manure based on EDEM. *Transactions of the CSAE*, 2020; 36(15): 95–102. (in Chinese)
- [19] Yao S Q, Shi G K, Wang B S, Peng H J, Meng H W, Kan Z. Calibration of the simulation parameters of jujubes in dwarfing and closer cultivation in Xinjiang during harvest period. *Int J Agric & Biol Eng*, 2022; 15(2): 256–264.
- [20] Chen T, Yi S J, Li Y F, Tao G X, Qu S M, Li R. Establishment of discrete element model and parameter calibration of alfalfa stem in budding stage. *Transactions of the CSAM*, 2023; 54(5): 91–100. (in Chinese)
- [21] Lenaerts B, Aertsen T, Tijskens E, Ketelaere B D, Ramon H, Baerdemaeker J D, et al. Simulation of grain-straw separation by discrete element modeling with bendable straw particles. *Computers and Electronics in Agriculture*, 2014; 101: 24–33.
- [22] Peng C W, Zhou T, Song S S, Fang Q, Zhu H Y, Sun S L. Measurement and analysis of restitution coefficient of black soldier fly larvae in collision models based on hertz contact theory. *Transactions of the CSAM*, 2021; 52(11): 125–134. (in Chinese)
- [23] Liao Y Y, You Y, Wang D C, Zhang X N, Zhang H F, Ma W P. Parameter calibration and experiment of discrete element model for mixed seeds of oat and arrow pea. *Transactions of the CSAM*, 2022; 53(8): 14–22. (in Chinese)
- [24] Zhang G Z, Chen L M, Liu H P, Dong Z, Zhang Q H, Zhou Y. Calibration and experiments of the discrete element simulation parameters for water chestnut. *Transactions of the CSAE*, 2022; 38(11): 41–50. (in Chinese)
- [25] Zhang S W, Zhang R Y, Cao Q Q, Zhang Y, Fu J, Wen X Y, et al. A calibration method for contact parameters of agricultural particle mixtures inspired by the Brazil nut effect (BNE): The case of tiger nut tuber-stem-soil mixture. *Computers and Electronics in Agriculture*, 2023; 212: 108112.
- [26] Shu C X, Yang J, Wan X Y, Yuan J C, Liao Y T, Liao Q X. Calibration and experiment of the discrete element simulation parameters of rape threshing mixture in combine harvester. *Transactions of the CSAE*, 2022; 38(9): 34–43. (in Chinese)
- [27] Zhong J Q, Tao L M, Li S P, Zhang B, Wang J Y, He Y L. Determination and interpretation of parameters of double-bud sugarcane model based on discrete element. *Computers and Electronics in Agriculture*, 2022; 203: 107428.
- [28] Wang S, Yu Z H, Aorigele, Zhang W J. Study on the modeling method of sunflower seed particles based on the discrete element method. *Computers and Electronics in Agriculture*, 2022; 198: 107012.